Sensors & Actuators: B. Chemical 275 (2018) 470–482

Contents lists available at ScienceDirect

Sensors and Actuators B: Chemical

journal homepage: www.elsevier.com/locate/snb

Using microfluidic impedance cytometry to measure *C. elegans* worms and identify their developmental stages

Zhen Zhu[a,*], Weijie Chen[a], Beitong Tian[a], Yulong Luo[a], Jianfeng Lan[b], Di Wu[b], Di Chen[b], Zixin Wang[c], Dejing Pan[d]

[a] Southeast University, Key Laboratory of MEMS of Ministry of Education, Sipailou 2, Nanjing 210096, China
[b] Nanjing University, Model Animal Research Center, Xuefu Road 12, Nanjing 210061, China
[c] Sun Yat-Sen University, School of Electronics and Information Technology, Xingang Xi Road 135, Guangzhou 510275, China
[d] Soochow University, Jiangsu Key Laboratory of Neuropsychiatric Diseases and Cambridge-Suda Genomic Resource Center, Ren-ai Road 199, Suzhou 215213, China

ARTICLE INFO

Keywords:
Microfluidic impedance cytometry
Electrical impedance spectroscopy
Caenorhabditis elegans
Developmental stage
Worm size

ABSTRACT

Microfluidic impedance cytometry allows for label-free detection of cells. But it has not yet been used to detect large organisms, such as *Caenorhabditis elegans* (*C. elegans*) worms, due to their variable morphology and strong motility. Here, we report on a *C. elegans* microfluidic impedance cytometry (*Ce*MIC), which enables the electrical impedance measurement of worms when flowing through a straight microchannel and the identification of their developmental stages based on impedance signals. With the optimized configuration of impedance-sensing structures, namely the microchannel and integrated microelectrodes, the influence of undulation and position variation of worms upon the measured impedance can be eliminated. In signal processing, a kernel density estimation method is employed to extract worm-length-related values that can be directly assigned to the developmental stages of worms. The accuracy for impedance-based identification of worm stages can reach 90%. Additionally, the *Ce*MIC device is developed into a simple and automated system for size-based enrichment of worms. Large and small worms from a mixed population are successfully separated to different outlets after identifying their sizes with impedance measurement. Therefore, our *Ce*MIC system provides a promising platform to measure the worm size, identify developmental stages, and prepare size/stage-homogenized populations for *C. elegans* experiments.

1. Introduction

Microfluidic impedance cytometry (MIC) allows for high-throughput, non-invasive and label-free detection of biological samples exposed to an electric field [1]. It is usually assembled by implementing electrical impedance spectroscopy (EIS) in a flow-through microfluidic device via microelectrodes. When cells pass through the sensing region between electrodes, their morphological and dielectric parameters, such as cell size, volume and membrane capacitance, can be detected. Thus, MIC has been always used to identify target cells from a homogenized population or classify a mixture of cells into subpopulations [2–7]. Recently, MIC has been involved in organ-on-a-chip systems to measure the size of spherical tissues and further evaluate their growth and response to drugs based on impedance signals [8,9]. However, MIC has not yet been used to detect large biological samples, such as *Caenorhabditis elegans*, due to their strong motility, variable morphology and widely-ranged size.

C. elegans, as a well-characterized model organism, has been widely used to understand genetic questions of developmental biology, aging and neurobiology [10]. Its life cycle consists of embryonic, larval and adult stages. After hatched from eggs, *C. elegans* enters the development that is comprised of four larval stages (L1, L2, L3 and L4) and adulthood. Each larval stage is ended with a molt that is used to separate the developmental stages. At each developmental stage, *C. elegans* features different body size, morphology and behavior [11–13]. As such, the developmental stages can be simply identified through the worm size.

Our previous studies in single-cell impedance measurement have shown that the impedance signal acquired from a MIC system is correlated to the volume of detected sample, even for a non-spherical one [14,15]. Since the size of *C. elegans* is vitally interrelated to its development, MIC holds the capabilities of precisely measuring the worm volume and further identifying its developmental stage. However, in the aforementioned MIC systems for cell sensing, microelectrodes were patterned closely to each other (in a distance from several microns to

* Corresponding author.
E-mail address: zhuzhen@seu.edu.cn (Z. Zhu).

https://doi.org/10.1016/j.snb.2018.07.169
Received 25 March 2018; Received in revised form 22 June 2018; Accepted 31 July 2018
Available online 06 August 2018

dozens of microns) due to the small size of cells. Thus, a peak was always displayed on the signal curve when a cell passed by, and then the signal difference was easily extracted by using a baseline-to-peak or peak-to-peak detection method to quantify the impedance contribution of the detected cell [6–8]. For the cylindrical and curved *C. elegans*, in comparison, its length varies from ~200 μm to ~1.2 mm and its body may undulate actively during perfusion in the microchannel. Any change of morphology or position that occurred to a worm when passing the sensing region may induce drastic variation of impedance signals. Therefore, the channel and electrode configuration and the signal processing methods in previous cell-based systems are not appropriate to *C. elegans* application.

In this work, we presented a MIC for *C. elegans* (namely *Ce*MIC) to perform the electrical impedance measurement of flow-through worms and subsequently identify their developmental stages with impedance signals. Based on the three-dimensional (3D) finite-element modeling of the impedance measurement of worms, we demonstrated that the optimum configuration of microchannel and microelectrodes in the *Ce*MIC device was suitable for the morphological features of *C. elegans* and can eliminate the influence of worm undulation upon the impedance measurement. Kernel density estimation, a nonparametric model in statistics for the estimation of probability density function of random variables, was employed to process impedance signals and calculate the baseline-to-plateau current in experiments. Thus, data that were correlated with worm length can be stably extracted to identify the developmental stages of *C. elegans*. Additionally, in order to study the potential applicability of the *Ce*MIC device, it was developed into a simple and automated system for size-based worm enrichment by integrating polydimethylsiloxane (PDMS) pneumatic valves and distributary channels downstream in the worm channel. With this system, large and small worms from a mixed population were identified through the impedance measurement and subsequently separated.

2. Materials and methods

2.1. Design of the microfluidic device (CeMIC)

Fig. 1 shows the *Ce*MIC device, which consists of a glass substrate, gold (Au) microelectrodes and two layers of PDMS (fluidic layer and control layer) for worm perfusion (worm channel) and pneumatic valve control (control channel), respectively. In order to perform the electrical impedance measurement and downstream enrichment of *C. elegans* worms, the *Ce*MIC system features two functions: measuring the flow-through worms by using microfluidic impedance cytometry and subsequently steering the identified worms to target outlets.

(i) Electrical impedance measurement of worms is achieved by integrating a pair of coplanar Au electrodes (i.e. stimulating and sensing electrodes) into a straight channel (Fig. 1). The channel is 160-μm wide and 130-μm high, and thus provides adequate space for worm perfusion, especially for adult worms, which have a length from ~900 μm to ~1.2 mm and a diameter from ~75 μm to ~100 μm [16,17]. The stimulating and sensing electrodes are 50-μm wide, 200-nm thick, and have a distance of 3000 μm. Once a worm enters and flows in the sensing region of the straight channel between electrodes, the impedance signal is supposed to vary drastically and then be maintained at a value until it flows out of the sensing region since the distance between electrodes is much longer than the length of any worm. The impedance variation can be measured by using an electrical impedance spectroscope and correlated with the volume of the detected worm. Concurrently, real-time video of each passing worm is recorded for optical measurement of worm length. *C. elegans* at each developmental stage features a specific range of worm length that results in distinct variation of impedance signals. Therefore, the developmental stages, which correlate to worm length, can be identified according to further analysis of impedance signals.

(ii) For the size-based enrichment of worms, two distributary channels downstream in the worm channel are constructed in a "Y-shaped" pattern and are connected to two outlets for collecting large and small worms, respectively. The distributary channels are controlled to open or close through pneumatic valves made of a thin layer of elastic PDMS membrane. When compressed air with a high pressure is applied to the control channel above one distributary channel, the PDMS membrane in between deforms (Fig. 1b), thereby blocking the outflow in the distributary channel. Worms are thus steered to flow in the other distributary channel towards its outlet. Moreover, it is important to note that a segment of meander channel is designed in the worm channel in order to extend the time duration of the worm flowing from the sensing region to the fork of "Y-shaped" distributary channels. This time extension can provide adequate time lag for the procedure of identifying and steering a worm, including the acquisition and real-time processing of impedance signals, the response of solenoid valve, and the activation of PDMS pneumatic valves.

2.2. Device fabrication and experimental setup

The microfluidic device was fabricated by bonding a double-layer PDMS stamp to a glass chip that has been metallized with Au microelectrodes. First, 150 nm Au with a 50-nm-thick titanium (Ti) layer underneath were deposited and patterned on a 4-inch glass wafer by using a lift-off process. The glass wafer was then diced into single chips for bonding later. Second, PDMS (Sylgard® 184, Dow Corning, USA) layers were fabricated by using standard soft lithography techniques. A 60-μm-thick layer of SU-8 3025 photoresist (MicroChem, USA) was spin-coated on a 4-inch silicon wafer to pattern a mold of control layer. On another silicon wafer, SU-8 3025 was spin-coated twice to form a 130-μm-thick layer followed by photolithography to obtain a mold of fluidic layer. Both molds were then coated with trichloro (1H,1H,2H,2H-perfluorooctyl)silane (Sigma-Aldrich, USA) in a vapor silanization process in order to prevent PDMS from adhering to SU-8 masters. Several drops of silanizing agent were placed on a glass slide, which was placed in a desiccator together with both SU-8 molds. The desiccator was then maintained under a vacuum at room temperature for about 2 h resulting in the silanizing agent to evaporate and form a monolayer on the surface of both molds. The SU-8 mold of control layer was transferred to PDMS with a mixture of 10:1 w/w base to curing agent ratio. To transfer the fluidic layer to PDMS with a thin membrane on top, a PDMS mixture of 20:1 was spin-coated on its SU-8 mold wafer to form a layer of about 200 μm thickness. Thus, a thin PDMS membrane of about 70 μm was realized for pneumatic valves. After cutting the PDMS control layer into chips, control channels on chips were first punched with holes as inlets for compressed air and were then bonded onto the upper surface of PDMS fluidic layer through oxygen plasma surface modification (PDC-002-HP, Harrick Plasma, USA). Afterwards, bonded PDMS stamps were peeled off from the SU-8 mold of fluidic layer and were punched with holes as inlet and outlets for worms. Finally, each PDMS stamp was irreversibly bonded to a glass chip diced before to accomplish the entire device fabrication.

The assembly of experimental setup is shown in Supplementary Fig. S1. (i) A *Ce*MIC device was clamped tightly between a custom-made aluminum (Al) holder and a polymethylmethacrylate (PMMA) cover by using plastic screws. (ii) A custom-made printed circuit board (PCB), comprising spring contact probes, SMA connectors and a microcontroller unit (MCU), was then placed above the PMMA cover. The spring probes contacted electrode pads on the device when screwed to the Al holder. (iii) For fluidic access, tubing, passing through holes in the PMMA cover, was directly inserted into the inlet and outlet holes on PDMS. The assembled setup was then placed on a stereomicroscope equipped with a camera for video recording. Connection between the assembled *Ce*MIC setup and the peripheral equipment is schematically illustrated in Fig. 1a. (iv) Mixed worms buffered in phosphate-buffered saline (PBS) solution were initially loaded into a syringe, and then continuously delivered to the worm channel at a flow rate of 30 μL/min

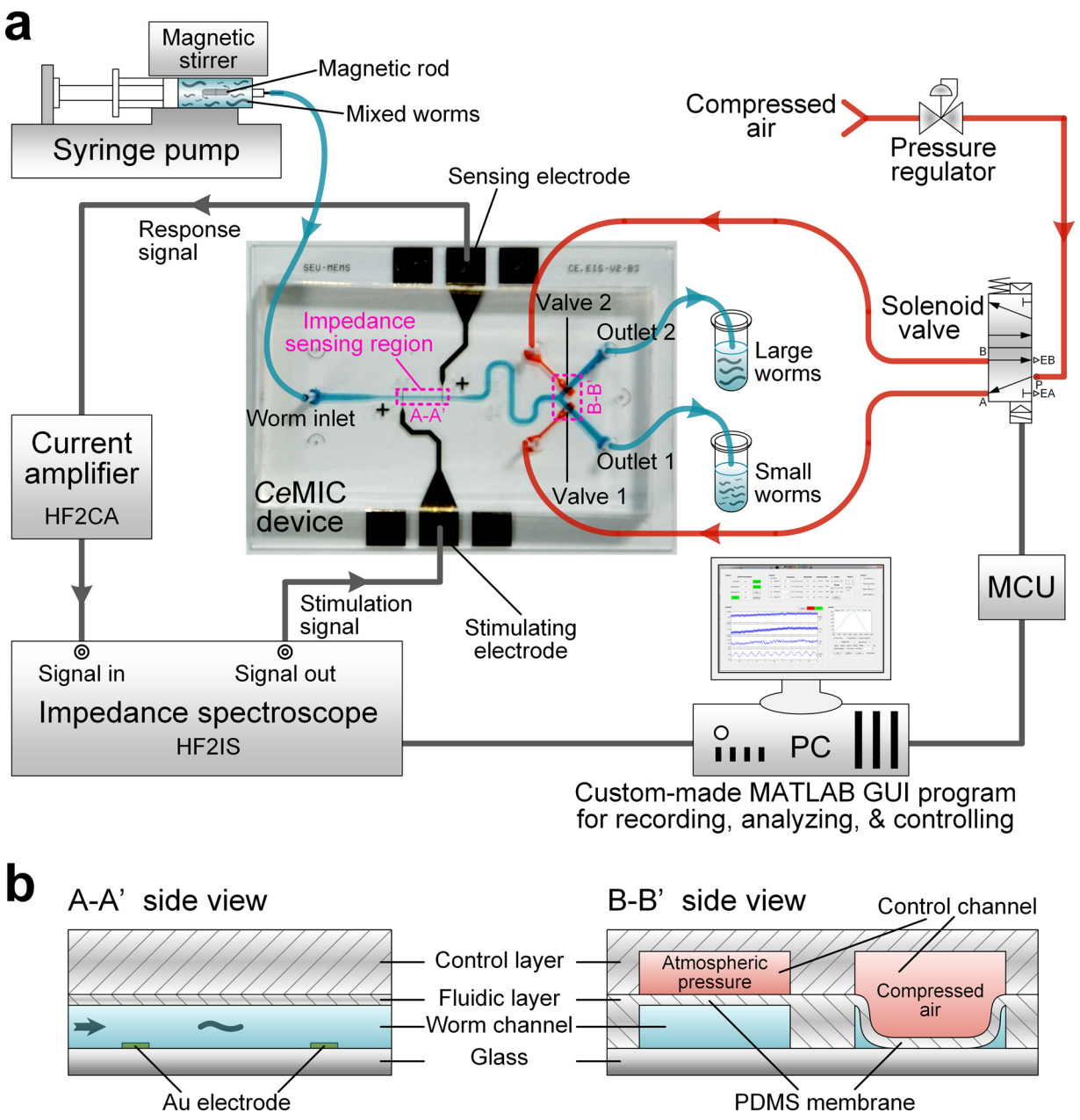

Fig. 1. *Ce*MIC system. (a) A photo of the *Ce*MIC device with schematically-illustrated peripheral equipment for the perfusion of *C. elegans* mixture, the electrical impedance measurement of flow-through *C. elegans* and the enrichment of stage-identified worms. (b) Cross sections of the sensing region (A-A') and the PDMS pneumatic valves (B-B').

by using a syringe pump (LSP02-2 A, Longer Precision Pump, China). To avoid the sedimentation of worms during delivery, a magnetic rod put in the syringe was used to stir the worm suspension through a mini magnetic stirrer. (v) A solenoid valve was connected to control channels through tubing and was supplied with compressed air regulated at a pressure of 150 kPa. The solenoid valve was controlled via the MCU to implement the activation and switching of pneumatic valves. (vi) For the impedance measurement of *C. elegans*, an electrical impedance spectroscope (HF2IS, Zurich Instruments, Switzerland) and a current amplifier (HF2CA, Zurich Instruments, Switzerland) were connected to the stimulating and sensing electrodes on the *Ce*MIC device via SMA connectors on the PCB. (vii) The impedance spectroscope and MCU were controlled with a custom-made MATLAB GUI (MathWorks, USA).

In addition, regarding the flow rate of worm perfusion during experiments, we have several considerations based on the performance of *Ce*MIC system. (i) When worms were passing through the 3000-μm-long sensing region, video was recorded for later on manual measurement of worm length and diameter from the extracted frames, which have to be clear enough. As a result, the flow rate cannot be set to a high value. (ii) The baseline-to-plateau detection of impedance signals was used to analyze worm events via Gaussian kernel density estimation (see Sections 2.4 and 3.2 for details), which required a certain length of signal plateau so that the event can be detected remarkably. As such, in order to create a signal plateau with a certain length, the flow rate cannot be very high. (iii) In the worm enrichment experiment using the *Ce*MIC system, adequate time delay after signal acquisition has to be provided for MATLAB signal analysis, solenoid valve switching, PDMS pneumatic valve activation, and the outflow of worm. These processes limited the applied flow rate. (iv) Due to the motility of worms, especially large worms (e.g. L4 and adult), some worms undulated strongly and even twined together, and they might be settled in the inlet or stack in the microchannel under a low flow rate. Therefore, we set the flow

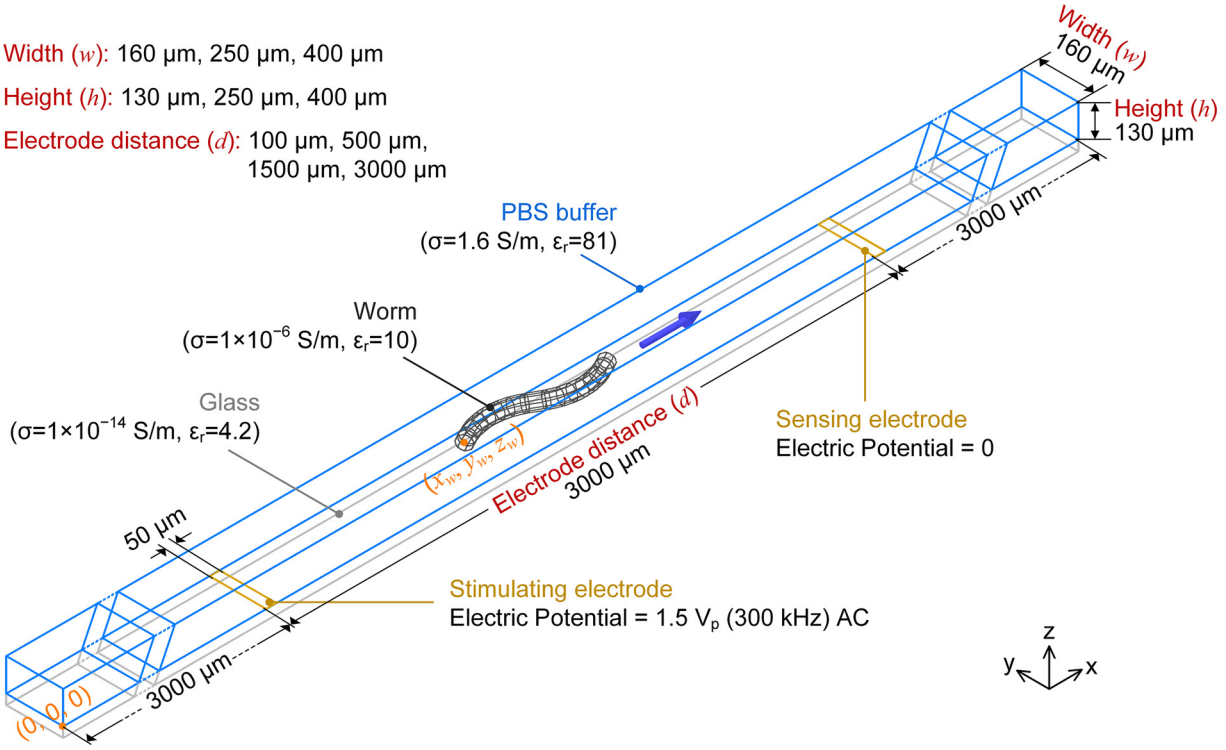

Fig. 2. 3D model geometry of microfluidic impedance cytometry for measuring flow-through *C. elegans* worms. The model structure consists of a glass substrate, a pair of stimulating and sensing electrodes, a worm channel filled with PBS medium, and a worm. The worm (x_w, y_w, z_w) is accurately positioned in the channel by defining its yz-coordinates (y_w, z_w) of the center of one end, while the worm flowing through the channel is imitated by varying its x-coordinate (x_w) at an interval of 50 μm along x-axis.

rate of worm perfusion to 30 μL/min, which brought an optimal performance of the *Ce*MIC system.

2.3. Modeling and simulation

A 3D finite-element model was established in COMSOL Multiphysics software (COMSOL, Inc., USA) to simulate the electrical impedance measurement of flow-through *C. elegans* in a microchannel. According to the impedance sensing structure in the *Ce*MIC device, the 3D model consists of Au electrodes, a straight channel filled with PBS medium and a worm passing through the channel. Fig. 2 shows the model geometry and lists the electrical conductivity (σ) and relative permittivity (ε_r) of materials (glass, PBS medium, and worm) used in simulation.

The geometric parameters are as follows: the channel length is 9000 μm; different values are set for the channel width (w: 160 μm, 250 μm and 400 μm) and channel height (h: 130 μm, 250 μm and 400 μm) to investigate the sensitivity of impedance measurement upon channel geometry; the stimulating and sensing electrodes have a width of 50 μm and a thickness of 0.2 μm; in order to study the influence of electrode distance on the impedance measurement of *C. elegans* worms, the distance between electrodes (d) are set to 100 μm, 500 μm, 1500 μm and 3000 μm, respectively; the worm (x_w, y_w, z_w) is accurately positioned in the channel by defining its yz-coordinates (y_w, z_w) of the center of one end, while the movement of worm along the channel is imitated by varying its x-coordinate (x_w) at an interval of 50 μm along x-axis. In simulation, we defined the representative lengths and diameters for worms at different developmental stages (L1-L4, and adult) and designed various shapes to mimic morphological changes induced by worm undulation. Curved worms were defined by using the sinusoid along x-axis (see Section 3.1 for details). Based on the numerical calculation of current density distribution, the resultant current on the sensing electrode was obtained at different geometric conditions and developmental stages of *C. elegans* worms.

In the model, a current conservation equation based on Ohm's law from the AC/DC module was applied. Boundary conditions and initial values were set as follows: exterior boundaries were set to "Electric Insulation"; interior boundaries at interfaces between different subdomains were set to "Continuity"; the domain of stimulating electrode was set to "Electric Potential" with an AC signal (amplitude 1.5 V at 300 kHz); the domain of sensing electrode was set to "Electric Potential" with a value of 0 V.

2.4. Electrical impedance measurement and data analysis

When worms were infused into the *Ce*MIC device, the electrical impedance measurement was carried out as follows: an alternative current (AC) signal (amplitude 1.5 V at 300 kHz) from the impedance spectroscope was applied to the stimulating electrode; the response signal from the sensing electrode was fed back via the current amplifier to the impedance spectroscope. The sampling rate was set to 1.8 kSa/s. The recorded signals in the characterization experiment were stored on a PC for later off-line analysis, while real-time signal acquisition and processing were performed in the enrichment experiment.

To characterize the relationship between the impedance signals and the developmental stages of *C. elegans*, the magnitude curve of stored current signals was divided into segments. Each segment, which exhibits the signal pattern of a detected worm, has a time duration of 1 s and includes 1800 sampling points accordingly. The data of each segment was then statistically analyzed by using Gaussian kernel density estimation (KDE) with adaptive bandwidth to estimate the probability density function (PDF) [18–21]. On the PDF curve, two noticeable peaks, representing the signal baseline and the worm event, respectively, can be found. Then, the signal variation (ΔI_{mag}) of a detected worm was simply calculated by subtraction between the current magnitude values corresponding to the two peaks. Furthermore, in the characterization experiment, real-time video was concurrently recorded

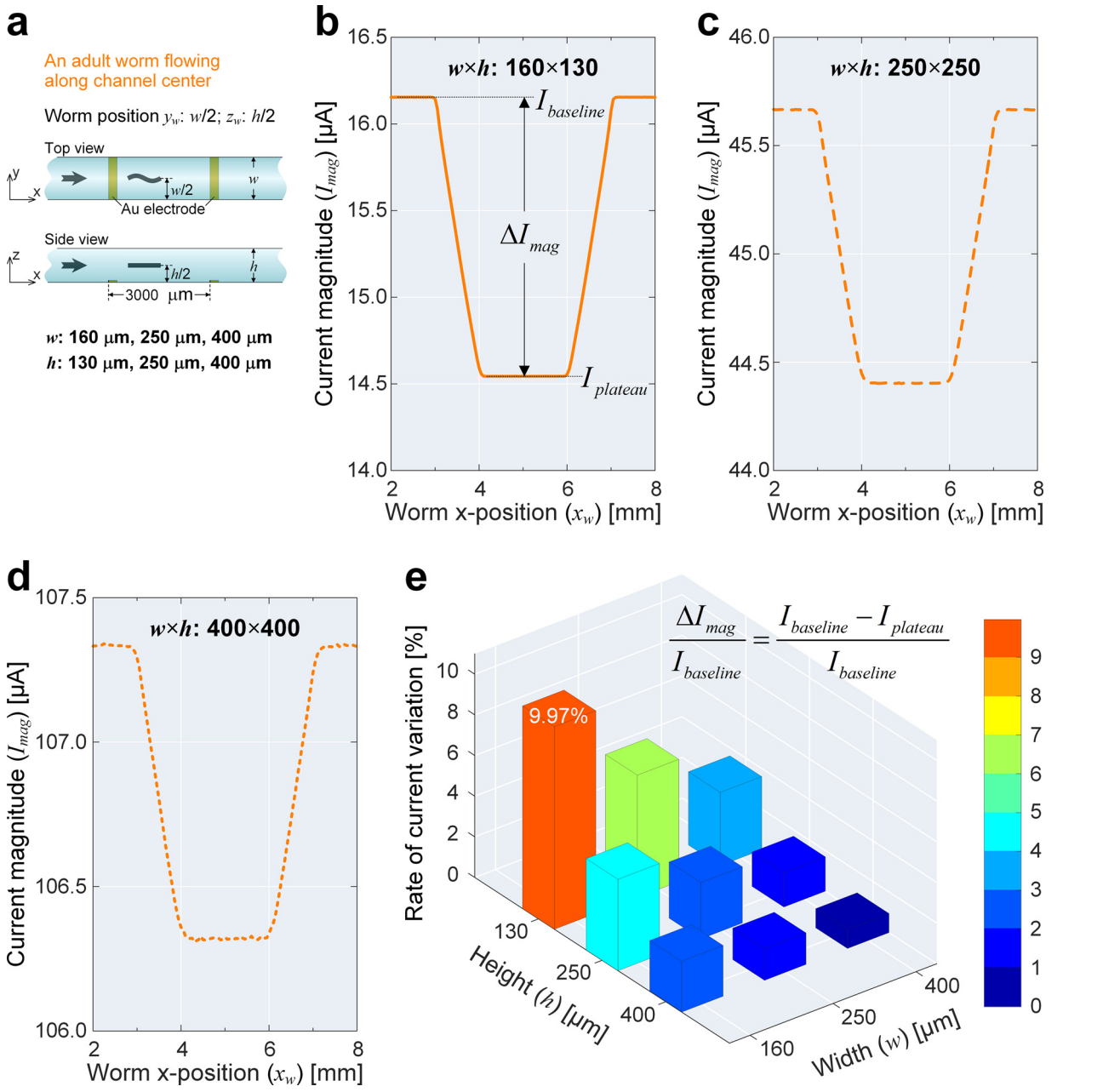

Fig. 3. Simulation of electrical impedance measurement in different channel geometry. (a) Top and side views of simulation model. Channel width w was set to 160 μm, 250 μm and 400 μm, respectively, and channel height h was set to 130 μm, 250 μm and 400 μm, respectively. Electrode distance d in the sensing region was fixed at 3000 μm. An "S-shaped" adult worm (ϕ-81 μm and L-1000 μm) flowing along the center line of channel was simulated. (b-d) Current magnitude curves of impedance measurement in three different channel dimensions. Current variation is defined as $\Delta I_{mag} = I_{baseline} - I_{plateau}$, where $I_{baseline}$ is the baseline current and $I_{plateau}$ is the current magnitude of signal plateau. (e) Rate of current variation $\frac{\Delta I_{mag}}{I_{baseline}}$ versus channel geometry.

when worms were passing the sensing region. Based on the images extracted from the video, optical length of each worm was measured manually in ImageJ/Fiji software (NIH, USA). Correlation between the optical length and the cubic root of ΔI_{mag} of detected worms was then calculated by means of linear regression. As worms have specific ranges of characteristic length in their life span, the developmental stages can be identified according to the definite values of impedance signal variations.

2.5. Worm enrichment

In the experiment of worm enrichment, the on-line recording and processing of impedance signals was implemented by using the custom-made program in MATLAB GUI. Prior to worm enrichment, the *Ce*MIC device was calibrated to obtain a correlation function between the acquired impedance signals and the developmental stages of worms. The calibration was performed in the same way as that used in the characterization experiment, however less worms were required in the calibration experiment for saving time. Based on the returned linear-regression function, threshold values of impedance signal variations for large worms (herein L4 and adulthood) were set in the GUI program. In order to perform the real-time data analysis, a sliding "window" of 1 s was set for signal acquisition. This window slid across the time series at an interval of 0.2 s. Statistical algorithms, the same as those used in the characterization, were employed in signal processing to look for the evidence of a detected worm. Initially, valve 1 on the *Ce*MIC device was open while valve 2 was closed, thereby collecting small worms (L1-L3) through outlet 1 (cf. Fig. 1a). Once the resultant $\sqrt[3]{\Delta I_{mag}}$ of a detected

worm was right in between the threshold values set before, the program transferred a feedback signal via the MCU to the solenoid valve to switch off valve 1 and to switch on valve 2 simultaneously. As a result, large worms were steered toward outlet 2 for sample collection.

2.6. C. elegans culture and preparation

Strains were cultured under standard laboratory condition as described [12]. *C. elegans* worms were cultured at 20 °C on Nematode Growth Medium (NGM) agar plates seeded with OP50 *Escherichia coli* as a food source. To perform the electrical impedance measurement of mixed *C. elegans*, non-synchronous worms at different developmental stages (L1-L4, and adult) were collected from the NGM plate and were then washed three times with M9 buffer to remove any residual bacteria. Finally, the mixed worms were suspended in PBS buffer for experiment.

3. Results and discussion

3.1. Modeling the electrical impedance measurement of flow-through worms

For *C. elegans*, its length ranges from ~200 μm to ~1.2 mm during its life cycle and its body undulates when flowing through the impedance sensing region in microchannel. Any morphological or position change of a worm may induce considerable variation of impedance signals. Therefore, in order to provide an optimum detection mechanism for *C. elegans*, the sensitivity of electrical impedance measurement upon the channel geometry and electrode configuration of the sensing region as well as the characteristics of measuring worms with the *Ce*MIC system were investigated through 3D finite-element modeling in COMSOL (Fig. 2). In simulation, representative diameters and lengths were defined for worms at five developmental stages: ϕ-25 μm and L-300 μm for L1, ϕ-37 μm and L-450 μm for L2, ϕ-45 μm and L-550 μm for L3, ϕ-61 μm and L-750 μm for L4, and ϕ-81 μm and L-1000 μm for adult [16].

3.1.1. Channel geometry

First, we simulated the electrical impedance measurement of an "S-shaped" adult worm flowing along the center line of microchannel through the sensing region (Fig. 3). The channel width and length were set to different values while the electrode distance was fixed (Fig. 3a). Fig. 3b–d shows the current magnitude curves which vary in the simulation of different channel dimensions. We can clearly see that the baseline current starts dropping when the worm approaches the stimulating electrode, and stays at a constant value (plateau) until the worm exits the sensing region. The rate of current variation $\frac{\Delta I_{mag}}{I_{baseline}}$, referring to the result of current difference between the baseline and plateau divided by the baseline current, was thus used to evaluate the impedance sensitivity upon channel geometry (Fig. 3e). In the case of the channel with a smallest cross-section of 160 μm × 130 μm among all simulated conditions, the rate of current variation reaches a highest value, 9.97%. Additionally, the channel width and height has to be larger than the diameter of adult worms so that they can flow through the sensing region smoothly without piling up in the microchannel. Therefore, the designed channel dimension ($w \times h$: 160 μm × 130 μm) of impedance sensing region in the *Ce*MIC device offers the optimum impedance sensitivity in measuring *C. elegans* worms, compared to channels with larger width and height.

3.1.2. Electrode distance and worm position

Next, we studied the influence of electrode distance and worm position on the impedance measurement of *C. elegans*. The channel cross-section was fixed at 160 μm × 130 μm, while the electrode distance was set to 100 μm, 500 μm, 1500 μm and 3000 μm, respectively (Fig. 4a). In simulation, an adult worm (ϕ-81 μm and L-1000 μm) shaped into an "S" form in x-y plane was positioned in the middle of channel to move along three trajectories: the center line (65 μm above the bottom), the lower midline (40.8 μm above the bottom) and the higher midline (40.8 μm under the top) of the channel, respectively. When the electrode distance is short (e.g. 100 μm and 500 μm, Fig. 4b,c), signal peaks display in the current magnitude curves. Thus, the impedance variation induced by the flow-through worm can be represented by the current difference between the signal baseline and the peak (baseline-to-peak current). In comparison, when the electrode distance (e.g. 1500 μm and 3000 μm, Fig. 4d,e) is longer than the worm length, the current difference between the signal baseline and the plateau (baseline-to-plateau current) is used to represent the impedance variation. Even through spikes at both ends of the plateau may appear on the signal curve as the worm approaching the electrode surface (flowing along the channel bottom), the signal plateau is still apparent for the baseline-to-plateau calculation.

Moreover, when electrodes are closely located (Fig. 4b,c), the current difference of the worm flowing along the channel bottom ΔI_{mag}^{CB} varies more drastically compared to that of the worm flowing along the channel center ΔI_{mag}^{CC} and that of the worm flowing along the channel top. However, in the case of that the electrode distance is long enough (Fig. 4d,e), the baseline-to-plateau current is maintained at a relatively constant value with limited disturbance from the change of worm positions. Accordingly, we calculated the rate of current variation by $\frac{\Delta I_{mag}^{CB} - \Delta I_{mag}^{CC}}{\Delta I_{mag}^{CC}}$, which refers to the result of the variation of current difference between the two cases of worm positions divided by the current difference of the worm flowing along the channel center. As shown in Fig. 4f, a longer distance between electrodes leads to a smaller rate of current variation. In particular, the impedance measurement by using electrodes with a distance of 100 μm causes a large rate of current variation, 122.57%, while the rate is diminished to 1.20% when the electrode distance is above 1500 μm. Hence, the impedance variation induced by the position change of a worm flowing through the sensing region can be eliminated by using a pair of electrodes that keep a relatively long distance from each other, and the baseline-to-plateau current can stably characterize the worm-induced signal variation. Considering that a short distance between electrodes results in a short signal plateau (Fig. 4d) and a long distance between electrodes may increase the chance to detect multiple worms simultaneously in the sensing region, herein, the electrode distance of our *Ce*MIC device is 3000 μm for the electrical impedance measurement of *C. elegans*.

3.1.3. Worm shapes

In addition, when worms were flowing in the microfluidic channel, some of them undulated randomly and some others behaved like cylinders. Such morphological variation of *C. elegans* during the movement was mimicked by using various shapes of worms in modeling. The cylindrical worm was modeled as a straight cylinder, and the undulated worms were modeled as curved ones. It is important to notice that curved worms were defined by using the sinusoid to simplify the geometric structure of undulated *C. elegans*. As illustrated in Fig. 5a, the diameter and length of worms at each developmental stage were fixed, but their shapes were varied to seven representative ones: straight, curved (0.5 sine, 1.0 sine and 1.5 sine) and vertically-curved (0.5 vertical sine, 1.0 vertical sine and 1.5 vertical sine), respectively. For simulated worms at each developmental stage, signal plateaus can be clearly observed on current magnitude curves, and their current values show no conspicuous change among different shapes of worms (Fig. 5b). The result demonstrates that such sensing mechanism in the *Ce*MIC device eliminates the influence of worm undulation on the electrical impedance measurement of flow-through *C. elegans*.

Furthermore, relationship between the baseline-to-plateau current ΔI_{mag} and the worm length at difference developmental stages was investigated by means of a linear regression calculation. Previous studies have proved that impedance signals obtained from microfluidic

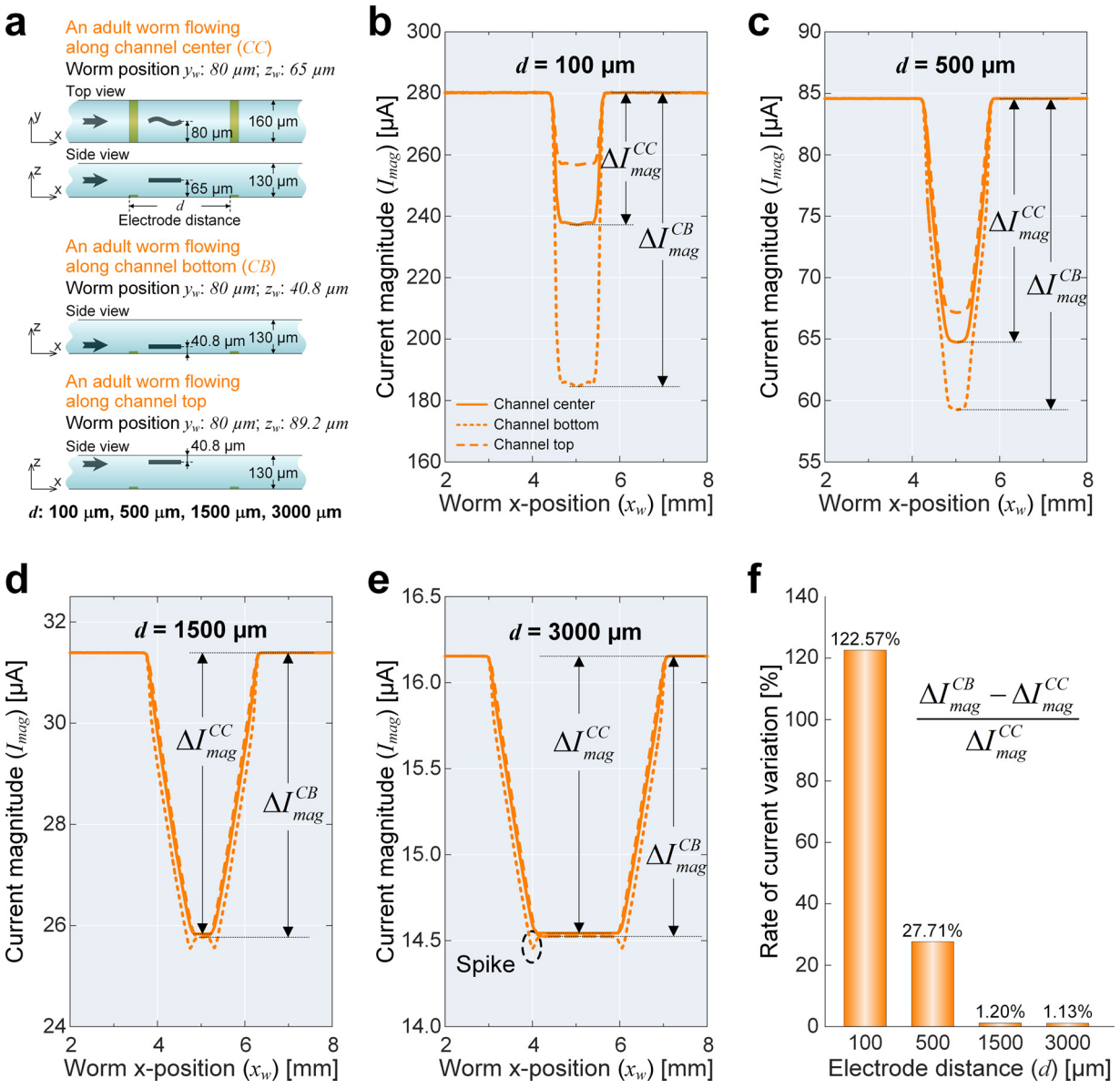

Fig. 4. Simulation of electrical impedance measurement with different electrode distance and worm position. (a) Top and side views of simulation model. Channel cross-section $w \times h$ was fixed at 160 μm × 130 μm. Electrode distance d in the sensing region was set to 100 μm, 500 μm, 1500 μm and 3000 μm, respectively. An "S-shaped" adult worm flowing along the center line of channel, the channel bottom and the channel top was simulated, respectively. (b-e) Current magnitude curves of impedance measurement with four different electrode distances and three different worm positions. Current variations of the worm flowing along the channel center

impedance cytometry are linearly correlated to the volume of measured samples [14,15,22,23]. Since the worm length are directly proportional to the diameter [16], worms at five representative developmental stages in modeling were defined as cylinders with linearly-correlated length and diameter. Thus, Fig. 5c shows a linear relationship between the cubic root of ΔI_{mag} and the worm length with a high coefficient of determination R^2 of 0.9995. This result suggests that our *Ce*MIC device enables the measurement of worm length and the identification of developmental stages by using impedance signals.

3.2. Characterizing the electrical impedance measurement of worms

In order to further investigate the capability and sensitivity of the *Ce*MIC system, we performed the characterization experiment. Fig. 6 shows the exemplary signal curves, images and corresponding PDF curves of measuring *C. elegans* worms at five different developmental stages (L1-L4 larval stages and adulthood). For a typical signal pattern of measuring a worm in the *Ce*MIC device, the current magnitude first undergoes a sudden drop from its baseline to a lower value, and subsequently maintains at this value until it rises back to the baseline. Similar patterns have been shown in Section 3.1, and thus the experimental and simulation results are in good agreement. The baseline signal refers to the impedance of an empty sensing region filled with PBS medium. The signal variation from the baseline to a lower current is attributed to the contribution of a worm to the measured impedance when the worm is detected in the sensing region. As the electrode distance (3000 μm) in the sensing region is longer than the length of worm, the signal variation can last for a short time duration, thereby forming a signal plateau. No matter a short larva at L1 stage with a length of 277.39 μm or a large adult worm with a length of 1186.21 μm, such signal pattern can be clearly observed on the current magnitude curves (cf. blue curves in Fig. 6). The signal drop occurs when the worm is approaching the stimulating electrode and leaving the sensing electrode, whilst the plateau occurs when the worm is flowing between

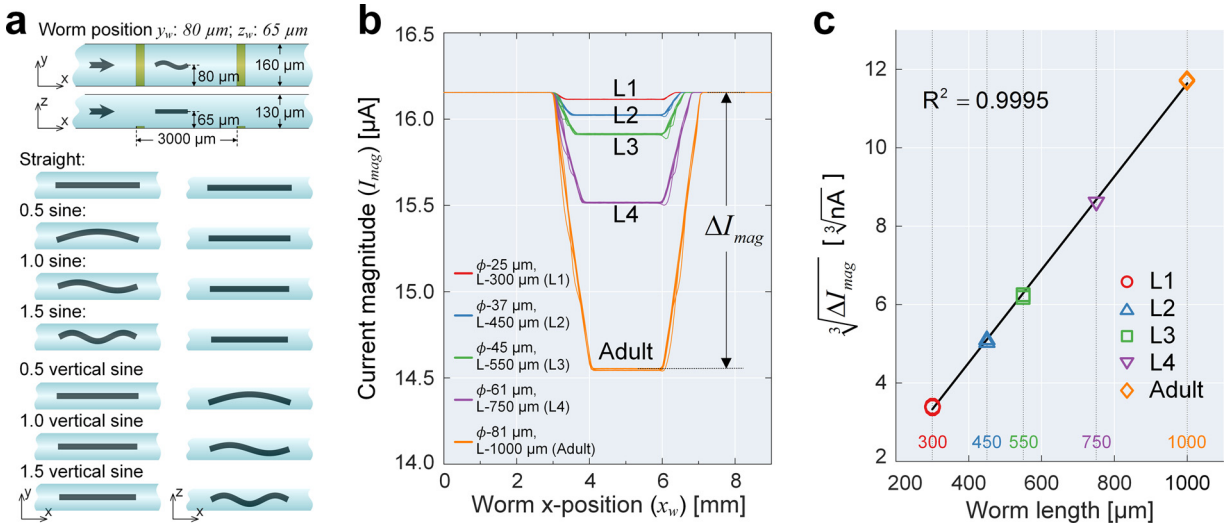

Fig. 5. Simulation of electrical impedance measurement of *C. elegans* worms at five developmental stages (L1-L4 and adult) with different morphology. (a) Top and side views of simulation model and worm morphology. Channel cross-section $w \times h$ was fixed at 160 μm × 130 μm, and electrode distance d was fixed at 3000 μm. All worms flowed along the center line of channel. Seven representative shapes of worms at each developmental stage were simulated: straight, curved (0.5 sine, 1.0 sine and 1.5 sine) and vertically-curved (0.5 vertical sine, 1.0 vertical sine and 1.5 vertical sine). (b) Current magnitude curves of worms at five developmental stages with seven different shapes. (c) Linear regression between the cubic root of baseline-to-plateau current $\sqrt[3]{\Delta I_{mag}}$ and the length of worms with seven different shapes.

electrodes.

To evaluate the impedance contribution of a worm to the empty sensing region, the current difference between the baseline and the plateau has to be calculated. Regarding the *Ce*MIC system that is applied later for the automatic enrichment of worms, the data analysis and computation has to be fast and precise. Herein, KDE is used to estimate the PDF from current magnitude values of all sampling points of each detected worm. Then, two remarkable peaks displayed on each PDF curve (cf. red curves in Fig. 6) can represent the maximum probability densities of the baseline and the plateau, respectively, and also correspond to the currents of the baseline and the plateau. Thus, the baseline-to-plateau current (ΔI_{mag}) of each detected worm can be simply calculated by the subtraction between the two current values. Five exemplary *C. elegans* worms at L1-, L2-, L3-, L4-larval and adult stages in Fig. 6 show different baseline-to-plateau currents of 6.08 nA, 11.86 nA, 32.70 nA, 67.23 nA and 220.70 nA, respectively. With the increase of worm length along the *C. elegans* development, the impedance contribution of the worm to the sensing region increases and the current that the sensing electrode receives decreases. As a result, an adult worm results in a higher baseline-to-plateau current than a short larva, such as a L1 worm.

Moreover, two noticeable spikes at both ends of the signal plateau can be observed on the current magnitude curves of some samples, for example, the L4 and adult worms in Fig. 6. Generation of the spikes could be attributed to the undulation and position variation of worms when flowing through the sensing region, as proved by simulation results (cf. Fig. 4d,e). *C. elegans*, unlike cells that can be dragged to flow stably during perfusion, may undulate actively in the microchannel and approach or even touch the surface of electrodes when entering and exiting the sensing region, and thus lead to a drastic change of electric current distribution. In the conventional cell-based microfluidic impedance cytometry, peak-to-peak or baseline-to-peak detection methods were commonly used to analyze the recorded current or voltage signals [6–8]. However, those methods are not applicable in this work for the sake of spikes on signal curves. In contrast, KDE method returns a PDF that contains all variables. Two significant variables, referring to the events of the signal baseline and the plateau, can be extracted. As the sampling points of spikes are always much less than those of the signal plateau, this method eliminates the disturbance of signal spikes in signal processing and offers a fast and precise detection method of the baseline-to-plateau current, ΔI_{mag}.

3.3. Identifying the developmental stages of C. elegans

According to the 3D finite-element modeling and the characterization experiment above, we have verified that the *Ce*MIC system is capable of the electrical impedance measurement of *C. elegans* and the impedance signals are correlated with the size of worms at different developmental stages. Herein, to identify the developmental stages of worms by using impedance signals, we measured about 800 worms in a mixed population by using the *Ce*MIC system. In the off-line data processing, the baseline-to-plateau current ΔI_{mag} of each detected worm was calculated from the recorded impedance signals via KDE algorithm, and meanwhile the optical length of each worm was measured from the recorded video. The correlation between the baseline-to-plateau current and the worm length was then investigated by means of a linear regression calculation. As shown in Fig. 7, the cubic root of ΔI_{mag} is linearly correlated to the optical length of worms, and the coefficient of determination R^2 reaches a high value of 0.97. For *C. elegans* worms, their length and diameter increase accordingly with their development and show a linear relationship in between (Supplementary Fig. S2) [16]. Approximating the worm as a cylinder, the cubic root of worm volume is proportional to the worm length. As proved in previous studies, impedance signals obtained from microfluidic impedance cytometry are linearly correlated with the volume of measured samples. Therefore, the linear relationship between the cubic root of baseline-to-plateau current and the worm length can be elucidated, and $\sqrt[3]{\Delta I_{mag}}$ can be used directly to characterize the worm length.

Since the development of *C. elegans* is interrelated to worm length, the measured impedance signals can be used to simply identify the developmental stages. Each larval stage is ended with a molt where a new cuticle is synthesized and the old one is shed [11,12]. The length of worm between the last and the next developmental stages is determined by the length at molt [13]. According to the literature [17], we used a linear interpolation between the lengths at each molt and defined the length thresholds at L1/L2, L2/L3, L3/L4 and L4/adult molt as 370 μm, 500 μm, 635 μm and 920 μm, respectively. Based on the returned equation of linear regression ($y = 0.0052x + 0.35$) and the corresponding threshold length of worms, four threshold values of $\sqrt[3]{\Delta I_{mag}}$ were obtained: 2.26, 2.93, 3.63 and 5.10, respectively. Using the four criteria to identify worm stages, each detected worm was assigned to

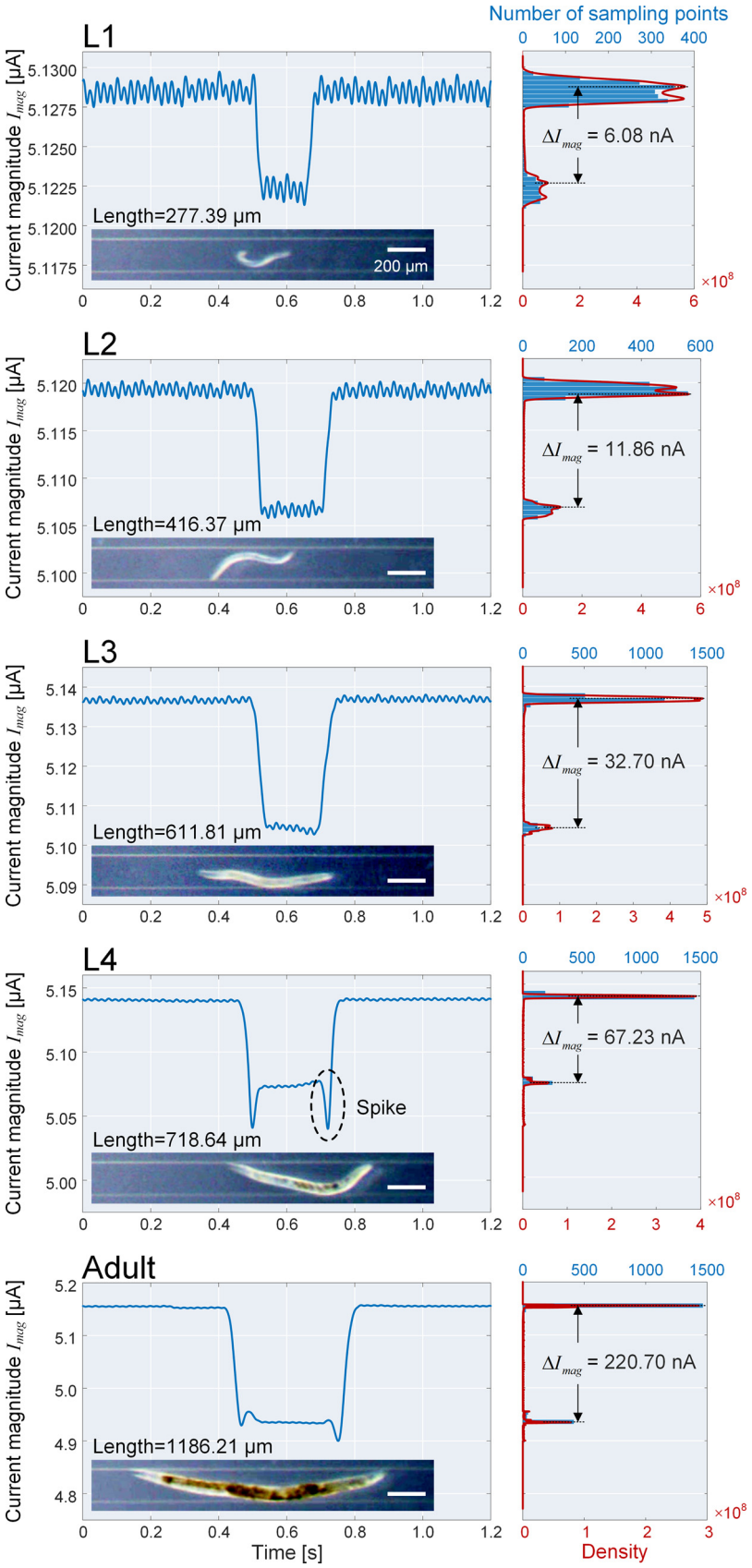

Fig. 6. Signal curves (blue) of current magnitude obtained from the impedance measurement of *C. elegans* worms at five representative stages (L1-L4 and adult) and PDF curves (red) obtained from the KDE analysis of corresponding current magnitude signals. Inserts show the images of worms corresponding to the recorded impedance signals. Scale bar is 200 μm. (For interpretation of the references to colour in this figure legend, the reader is referred to the web version of this article).

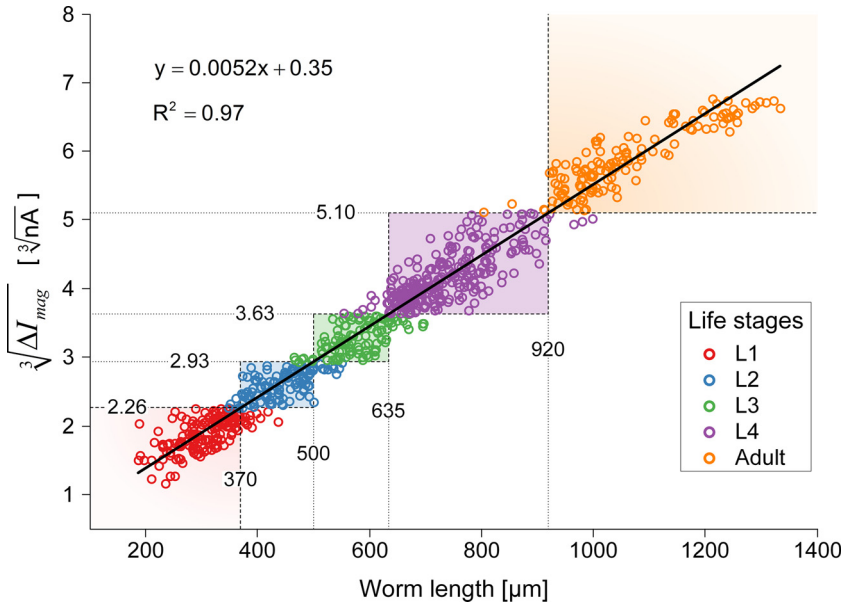

Fig. 7. Identification of *C. elegans* developmental stages based on impedance signals. The cubic root of baseline-to-plateau current, $\sqrt[3]{\Delta I_{mag}}$, is linearly correlated with the worm length. According to the definite worm length at molt between two continuous stages (370 μm for L1/L2, 500 μm for L2/L3, 635 μm for L3/L4 and 920 μm for L4/adult), threshold values of $\sqrt[3]{\Delta I_{mag}}$ are used to classify worms into five groups (circles plotted in five different colors). The correctly-identified worms at each developmental stage refer to the data circles located in the corresponding light-colored box.

one of the five developmental stages (L1-L4 and adulthood) based on its impedance signal. As a result, detected worms were successfully classified into five stages marked in different colors (Fig. 7).

Furthermore, the accuracy for impedance-based identification of worm stages was evaluated. The actual developmental stage of each worm was examined by using optical length. Some worms were assigned to a specific developmental stage according to the impedance-based identification, but were mismatched with the length-identified stage. Therefore, the correctly-identified worm was the one assigned to the same developmental stage by using both impedance signals and optical length. The accuracy of impedance-based worm identification at each stage was then defined as the ratio of the number of correctly-identified worms (data located in each light-colored box in Fig. 7) to the number of worms classified by using impedance signals (data illustrated in the same color in Fig. 7). Table 1 shows the accuracy in identifying the developmental stages of worms measured with the *Ce*MIC. The average accuracy is above 90%, while it is even above 95% for large worms at L4-larval and adulthood stages. Hence, the experimental result demonstrates that the *Ce*MIC system features high accuracy in identifying the developmental stages of *C. elegans* through electrical impedance measurement.

3.4. Enrichment of worms using CeMIC

In addition, we used the *Ce*MIC system to separate *C. elegans* worms for the size-based enrichment. After measuring the worm length with the microfluidic impedance cytometry, large (i.e. L4 and adulthood) and small worms (i.e. L1-L3) from a mixed population were steered to the desired outlets through two distributary channels, respectively. The time-stacked images in Fig. 8a show the dynamic process of identifying a large worm and subsequently steering it to its outlet. When the worm was passing the sensing region (position 1), the electrical impedance spectroscope acquired real-time current signals that were immediately processed to determine the worm length. From position 1 to position 4, valve 2 was closed while valve 1 was open. During this time period, the medium flowed towards outlet 1 that collected small worms. After identifying the detected worm as a large one, instructions were transmitted via the MCU to the solenoid valve to switch on valve 2 and meanwhile to switch off valve 1. Since the moment of position 5, the distributary channel activated via valve 2 became free to deliver medium towards outlet 2 for the collection of the identified large worm. After enrichment, the collected worms were seeded on NGM agar plates. As exemplarily shown in Fig. 8b,c, worms from outlet 2 were mostly large while worms from outlet 1 were mainly small.

In order to test whether the *Ce*MIC system was harmful to worms after the enrichment experiment, we observed the collected worms on NGM agar plates via microscopy, and compared them with the control worms that did not flow through the *Ce*MIC system. We did not find any obvious morphological or behavioral differences between the enriched and control worms, and also, we did not find any dead worm according to the optical observation of worm locomotion. Worms started wiggling their bodies immediately and large worms even started laying eggs, as shown in Fig. 8b,c. Moreover, COPAS BioSorter and previous microfluidic devices [24,25] have demonstrated that the flow stress resulting from the perfusion through these devices has no harmful effect on worm viability and behaviors, even though higher flow rates were applied in these devices than that of the *Ce*MIC system. In addition, previous studies have shown that an electric field lower than 12 V/cm was harmless to the activity of *C. elegans* [26,27]. In this work, the electric field was lower than 10 V/cm (3 V_{pp} AC voltage, 3000 μm electrode distance) and was applied within a very short time period when the worm flowing through the sensing region. Therefore, the aforementioned results and facts confirmed that the *Ce*MIC system has no adverse effect on the activity of worms during the impedance measurement and

Table 1
Accuracy in identifying the developmental stages of *C. elegans* by using impedance signals.

Life stages & length ranges	L1 < 370 μm	L2 370-500 μm	L3 500-635 μm	L4 635-920 μm	Adult > 920 μm
Detected samples	155	116	109	277	137
Correct samples	144	102	89	264	133
Accuracy [%]	92.90	87.93	81.65	95.31	97.08

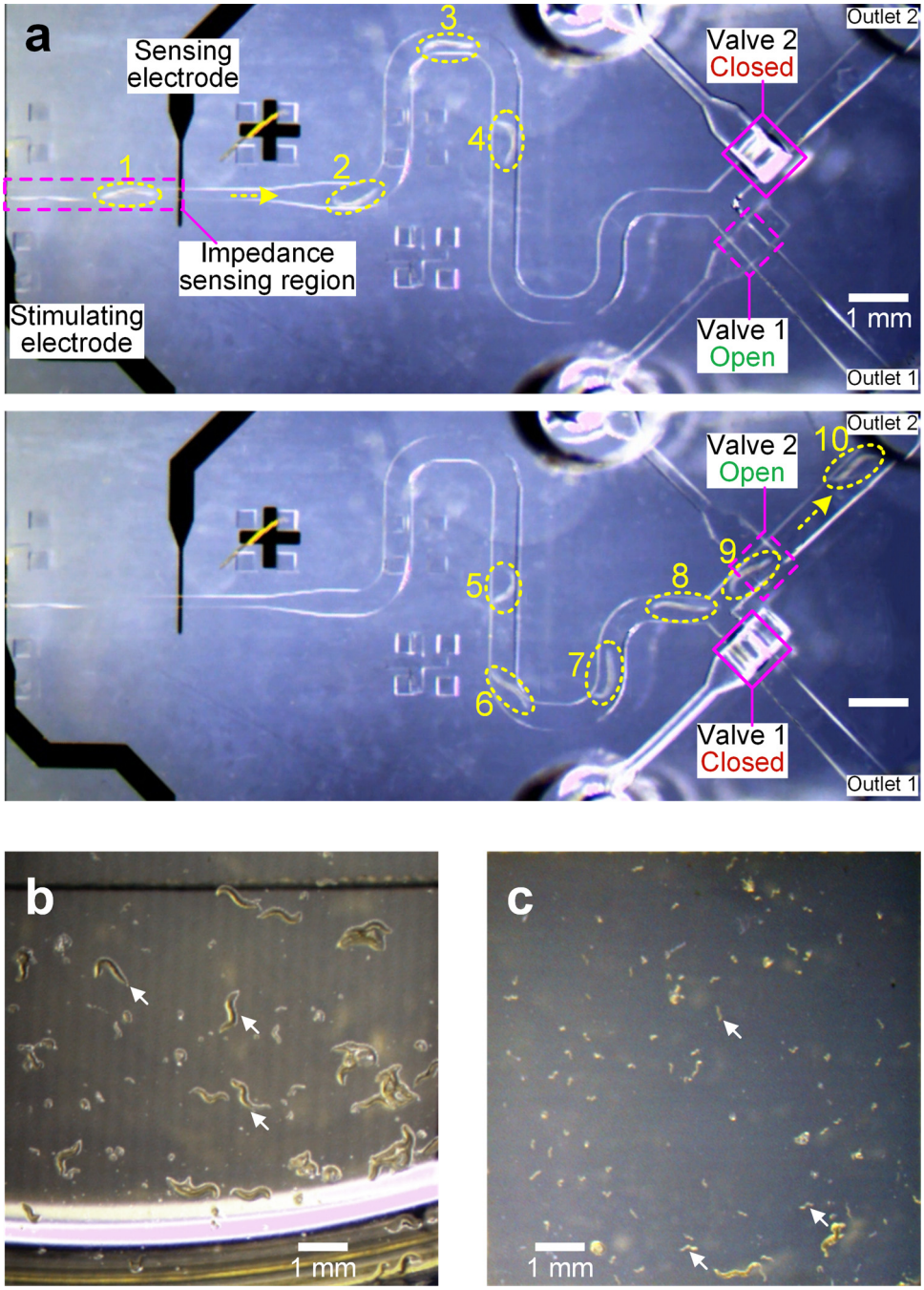

Fig. 8. Enrichment of *C. elegan* worms with the *Ce*MIC system. (a) Time-stacked images showing the dynamic process of steering a large worm for sample collection, including the movement of worm in the microchannel and the valve switching after identifying the worm as a large one. (b) Large and (c) small worms seeded on agar plates. They were collected from outlets 2 and 1, respectively. Scale bar is 1 mm.

enrichment.

Indeed, there were some worms separated by mistake, as can be seen in Fig. 8b,c. It can be elucidated by following reasons. (i) The motility of small *C. elegans* larvae was weaker than that of large worms. Small worms usually swam with the stream during perfusion, whilst large worms (e.g. L4 and adult) undulated strongly and even swam against the flow. Therefore, some small worms flowing in the microchannel may catch up with large ones and flow towards the wrong outlet. (ii) Although the PDMS membrane is elastic, its deformation cannot completely block the rectangular distributary channels (cf. Fig. 1b). As a result, small worms may squeeze through the narrow gap between the deformed membrane and the channel wall. (iii) The automation system for impedance signal processing and feedback control was simply designed and programmed. Once the signal pattern of a worm was detected via the *Ce*MIC system, the signal acquisition was paused for one second until the detected worm was identified and flowed out. During the halt of signal acquisition, some worms may pass through the sensing region without being detected. Such worms may follow the previously-identified worm to flow out, thereby causing the mistake of separation.

4. Conclusion

This work has presented a microfluidic impedance cytometry, *Ce*MIC, which enables the electrical impedance measurement of *C. elegans* worms when flowing through the sensing region between

electrodes. Compared with the conventional MIC for cells, here the configuration of microchannel and electrodes for impedance sensing has been optimized via 3D finite-element modeling for the application of cylindrical and undulated *C. elegans*. Namely, the channel dimensions have been designed to fit the morphology and behavior of worms, and the distance between coplanar electrodes has been extended to 3000 μm so that a plateau can always appear on the impedance signal curve when a worm passing the sensing region. Similar signal patterns have been obtained from both 3D simulation and characterization experiment. The results have demonstrated that the impedance sensing configuration as well as the baseline-to-plateau detection of impedance signals can eliminate the influence of undulation and position variation of worms upon the impedance measurement.

Since the approach of worms towards the electrode surface may induce drastic spikes at the ends of signal plateau, conventional algorithms for signal processing in cell-based MIC, such as baseline-to-peak or peak-to-peak detection are not applicable here. Alternatively, Gaussian kernel density estimation has been employed to efficiently extract the baseline-to-plateau current. According to the experimental results, we have unveiled a linear relationship between the cubic root of baseline-to-plateau current and the worm length, which relies on the development of *C. elegans*. The developmental stages (L1-L4 and adulthood) of worms have been simply identified through the measured impedance signals, leading to a high accuracy above 90%. As such, the *Ce*MIC system features accurate impedance measurement of flow-through *C. elegans* worms and identification of their developmental stages based on impedance signals.

Additionally, the *Ce*MIC device has been developed into a simple and automated system for the size-based enrichment of worms. By switching the outflow channel of worms with PDMS pneumatic valves, identified worms can be steered towards the desired outlets for collection. In the proof-of-concept experiment of worm enrichment, large and small worms have been first identified on-line through the real-time impedance measurement and subsequently separated to flow towards two outlets of the *Ce*MIC device with a throughput of about 30 worms per minute. Although some worms have been separated mistakenly, several practical solutions could be used in the future study to potentially improve the performance of the automated *Ce*MIC system in worm detection and enrichment. (i) As large worms are usually required for routine *C. elegans* experiments, small worms from a mixed population could be filtered off through net prior to sample loading. (ii) To eliminate the worm undulation, worms could converge in line under sheath-flow focusing, and then be oriented lengthways into a mostly straight configuration and flow through the microchannel one by one. Such a high-flow-rate condition requires that the channel length between the sensing region and the distributary channels has to be extended in order to provide sufficient time delay for signal processing, solenoid valve switching and PDMS pneumatic valve activation. (iii) In order to ultimately perform a simultaneous separation of worms with five stages from a mixed population, four *Ce*MIC devices could be cascaded sequentially so that adult worms could be isolated from the first device, then the rest will flow through the second device for the enrichment of L4 worms, and so on, until L1 and L2 worms could be separated in the fourth device. Such a complex setup requires more improvement and optimization on the robustness and stability of the operating system and data analysis algorithm in the future study. (iv) Optimizing both program and setup of the automated system, for example, accelerating the data acquisition and computation, using high-speed solenoid valve and shortening the response time of pneumatic valve, could benefit the improvement of the speed and yield of worm analysis and separation.

Moreover, we have compared the *Ce*MIC system with reported methods and devices for *C. elegans* sorting in terms of working principles, efficiency and features (Supplementary Table S1). These methods and devices include hand picking, commercial COPAS BioSorter, and microfluidic systems, such as electrotaxis-based and flow-filtration-based devices and our *Ce*MIC system. Hand picking is based on the operator's observation under stereomicroscopy, and thus it is labor-intensive and time-consuming. The output is highly dependent on individuals' operation. The commercial COPAS BioSorter is a high-throughput and automated instrument in worm sorting, but it is not affordable for most research laboratories and requires sophisticated operation and maintenance. Electrotaxis microfluidic devices are based on the phenomenon that worms swim towards negative electric field and worms at different developmental stages swim towards different deflecting angles under a constant electric field [26–29]. However, electrotaxis-implemented microfluidic devices have a trade-off between the throughput and accuracy in worm sorting and the mechanism has not been fully investigated. Flow-filtration microfluidic systems with a reasonably high throughput are based on size-variable microstructures, such as channels or pillars as filters [25,30–32]. However, such systems usually require custom-made complex microstructures. In comparison, the *Ce*MIC system is an active method like hand picking and COPAS BioSorter. It is automated without the requirement of intensive labor, low-cost and easy-to-use. It is based on the label-free electrical impedance spectroscopy and has a throughput of about 30 worms per minute, which is comparable to the efficiency of hand picking and electrotaxis-based microfluidic devices. Compared with flow-filtration systems, the *Ce*MIC system has simple and straightforward microfluidic configurations, which could be potentially improved into a more controllable and versatile system. Therefore, we believe that the *Ce*MIC system could be a potential platform to separate worms with specific size or developmental stages by further optimization on the design and operation of the system. Such platform could be employed for *C. elegans* research in developmental biology and aging.

Conflicts of interest

There are no conflicts of interest to declare.

Acknowledgments

This work was supported by the National Natural Science Foundation of China (No. 61774036, 31771299), the National Key Basic Research Program of China (No. 2015CB352100), and the Fundamental Research Funds for the Central Universities. We would like to thank Prof. Carlos Escobedo from Queen's University, Canada, for critical reading of the manuscript.

Appendix A. Supplementary data

Supplementary material related to this article can be found, in the online version, at doi:https://doi.org/10.1016/j.snb.2018.07.169.

References

[1] T. Sun, H. Morgan, Single-cell microfluidic impedance cytometry: a review, Microfluid. Nanofluid. 8 (2010) 423–443.
[2] D. Holmes, D. Pettigrew, C.H. Reccius, J.D. Gwyer, C. van Berkel, J. Holloway, D.E. Davies, H. Morgan, Leukocyte analysis and differentiation using high speed microfluidic single cell impedance cytometry, Lab Chip 9 (2009) 2881–2889.
[3] H. Song, Y. Wang, J.M. Rosano, B. Prabhakarpandian, C. Garson, K. Pant, E. Lai, A microfluidic impedance flow cytometer for identification of differentiation state of stem cells, Lab Chip 13 (2013) 2300–2310.
[4] M. Evander, A.J. Ricco, J. Morser, G.T.A. Kovacs, L.L.K. Leung, L. Giovangrandi, Microfluidic impedance cytometer for platelet analysis, Lab Chip 13 (2013) 722–729.
[5] N. Haandbaek, O. With, S.C. Burgel, F. Heer, A. Hierlemann, Resonance-enhanced microfluidic impedance cytometer for detection of single bacteria, Lab Chip 14 (2014) 3313–3324.
[6] M. Shaker, L. Colella, F. Caselli, P. Bisegna, P. Renaud, An impedance-based flow microcytometer for single cell morphology discrimination, Lab Chip 14 (2014) 2548–2555.
[7] B. de Wagenaar, S. Dekker, H.L. de Boer, J.G. Bomer, W. Olthuis, A. van den Berg, L.I. Segerink, Towards microfluidic sperm refinement: impedance-based analysis and sorting of sperm cells, Lab Chip 16 (2016) 1514–1522.

[8] S.C. Bürgel, L. Diener, O. Frey, J.-Y. Kim, A. Hierlemann, Automated, multiplexed electrical impedance spectroscopy platform for continuous monitoring of microtissue spheroids, Anal. Chem. 88 (2016) 10876–10883.
[9] Y.R.F. Schmid, S.C. Bürgel, P.M. Misun, A. Hierlemann, O. Frey, Electrical impedance spectroscopy for microtissue spheroid analysis in hanging-drop networks, ACS Sens. 1 (2016) 1028–1035.
[10] C.J. Kenyon, The genetics of ageing, Nature 464 (2010) 504–512.
[11] S. Brenner, The genetics of behaviour, Br. Med. Bull. 29 (1973) 269–271.
[12] S. Brenner, The genetics of Caenorhabditis elegans, Genetics 77 (1974) 71–94.
[13] L. Byerly, R.C. Cassada, R.L. Russell, The life cycle of the nematode Caenorhabditis elegans, Dev. Biol. 51 (1976) 23–33.
[14] Z. Zhu, X. Xu, L. Fang, D. Pan, Q.-A. Huang, Investigation of geometry-dependent sensing characteristics of microfluidic electrical impedance spectroscopy through modeling and simulation, Sens. Actuators B—Chem. 235 (2016) 515–524.
[15] W. Chen, B. Tian, J. Lan, D. Chen, Z. Zhu, Using microfluidic impedance cytometry to identify the life stages of *C. elegans* nematodes, IEEE Transducers 2017 (2017).
[16] B.T. Moore, J.M. Jordan, L.R. Baugh, WormSizer: high-throughput analysis of nematode size and shape, PLoS One 8 (2013) e57142.
[17] Z.F. Altun, D.H. Hall, Handbook of *C. elegans* anatomy. *WormAtlas*, Figure 6. Available at (2012) www.wormatlas.org/hermaphrodite/hermaphroditehomepage.htm.
[18] N. Agarwal, N.R. Aluru, A data-driven stochastic collocation approach for uncertainty quantification in MEMS, Int. J. Numer. Anal. Methods Eng. 83 (2010) 575–597.
[19] N.-B. Heidenreich, A. Schindler, S. Sperlich, Bandwidth selection for kernel density estimation: a review of fully automatic selectors, AstA—Adv. Stat. Anal. 97 (2013) 403–433.
[20] X. Xu, Z. Yan, S. Xu, Estimating wind speed probability distribution by diffusion-based kernel density method, Electr. Pow. Syst. Res. 121 (2015) 28–37.
[21] Z.I. Botev, J.F. Grotowski, D.P. Kroese, Kernel density estimation via diffusion, Ann. Statist. 38 (2010) 2916–2957.
[22] S. Gawad, K. Cheung, U. Seger, A. Bertsch, P. Renaud, Dielectric spectroscopy in a micromachined flow cytometer: theoretical and practical considerations, Lab Chip 4 (2004) 241–251.
[23] C. Bernabini, D. Holmes, H. Morgan, Micro-impedance cytometry for detection and analysis of micron-sized particles and bacteria, Lab Chip 11 (2011) 407–412.
[24] Y. Yan, L.F. Ng, L.T. Ng, K.B. Choi, J. Gruber, A.A. Bettiol, N.V. Thakor, A continuous-flow *C. elegans* sorting system with integrated optical fiber detection and laminar flow switching, Lab Chip 14 (2014) 4000–4006.
[25] X. Ai, W. Zhuo, Q. Liang, P.T. McGrath, H. Lu, A high-throughput device for size based separation of *C. elegans* developmental stages, Lab Chip 14 (2014) 1746–1752.
[26] P. Rezai, A. Siddiqui, P.R. Selvaganapathy, B.P. Gupta, Electrotaxis of *Caenorhabditis elegans* in a microfluidic environment, Lab Chip 10 (2010) 220–226.
[27] P. Rezai, S. Salam, P.R. Selvaganapathy, B.P. Gupta, Electrical sorting of Caenorhabditis elegans, Lab Chip 12 (2012) 1831–1840.
[28] B. Han, D. Kim, U. Hyun Ko, J.H. Shin, A sorting strategy for *C. elegans* based on size-dependent motility and electrotaxis in a micro-structured channel, Lab Chip 12 (2012) 4128–4134.
[29] X. Wang, R. Hu, A. Ge, L. Hu, S. Wang, X. Feng, W. Du, B.-F. Liu, Highly efficient microfluidic sorting device for synchronizing developmental stages of *C. elegans* based on deflecting electrotaxis, Lab Chip 15 (2015) 2513–2521.
[30] X.Ci. Solvas, F.M. Geier, A.M. Leroi, J.G. Bundy, J.B. Edel, A.J. deMello, High-throughput age synchronisation of *Caenorhabditis elegans*, Chem. Commun. (Camb.) 47 (2011) 9801–9803.
[31] L. Dong, M. Cornaglia, T. Lehnert, M.A.M. Gijs, Versatile size-dependent sorting of *C. elegans* nematodes and embryos using a tunable microfluidic filter structure, Lab Chip 16 (2016) 574–585.
[32] L. Yang, T. Hong, Y. Zhang, J.G.S. Arriola, B.L. Nelms, R. Mu, D. Li, A microfluidic diode for sorting and immobilization of Caenorhabditis elegans, Biomed. Microdevices 19 (2017) 38.

Zhen Zhu is currently Associate Professor at the School of Electronic Science and Engineering, Southeast University, China. He received a BSc and MSc in electronic engineering at Southeast University in 2006 and 2008, respectively. He received his Ph.D. in bioengineering from the Department of Biosystems, Science and Engineering (D-BSSE), ETH Zurich, Switzerland in 2014. His current research focuses on the integration of microfluidics, microsystems, and electronics for biomedical applications.

Weijie Chen received his BSc degree in electronic engineering from the School of Electronic Science and Engineering, Southeast University, China in 2017. He is currently pursuing his MSc degree at University of Wisconsin-Madison, USA.

Beitong Tian received his BSc degree in electronic engineering from the School of Electronic Science and Engineering, Southeast University, China in 2017. He is currently pursuing his MSc degree at Cornell University, USA.

Yulong Luo received his BSc degree in electronic engineering from the School of Electronic Science and Engineering, Southeast University, China in 2018. He is currently pursuing his MSc degree at Waseda University, Japan.

Jianfeng Lan received his BSc degree in biotechnology from Guangxi University, China in 2012. Currently he is a Ph.D. student in genetics at Nanjing University, China. His research focuses on functional genomics analysis of mutations that delay aging using *C. elegans*.

Di Wu received her BSc degree in biotechnology from Xinxiang Medical University, China in 2014. Currently she is a Ph.D. student in genetics at Nanjing University, China. Her work includes exploring roles of lipid metabolism in aging using *C. elegans*.

Di Chen received his BSc degree in marine biology from Ocean University of Qingdao, China in 1997, MSc degree in molecular genetics from Shanghai Institute of Plant Physiology, Chinese Academy of Sciences, China in 2000, and Ph.D. in genetics from University of Missouri-Columbia, USA in 2004. He is currently Associate Professor at Model Animal Research Center, Nanjing University, China. His group is using *C. elegans* as a model to explore the basic biology of aging.

Zixin Wang received a BSc, MSc and Ph.D. in opto-electronics engineering from Sun Yat-Sen University, China in 2000, 2003 and 2006, respectively. He is currently Associate Professor at the School of Electronics and Information Technology, Sun Yat-Sen University. His research focuses on the lock-in amplifier and electrical impedance spectroscopy.

Dejing Pan received a BSc and MSc in biochemistry at Sun Yat-Sen University, China in 1998 and 2001, respectively. He was awarded a Ph.D. in biomedicine by the Department of Biomedicine, University of Basel, Switzerland in 2008. He is currently Associate Professor at Jiangsu Key Laboratory of Neuropsychiatric Diseases and Cambridge-Suda Genomic Resource Center, Soochow University, China. His research focuses on the cell and medical biology and its interaction with organic interface in material and engineering science.